DUAL FREQUENCY BROADBAND REFLECTARRAY ELEMENT DESIGN

Norbahiah Misran[1] and Robert Cahill[2]

[1]*Electrical, Electronic and System Engineering Department Faculty of Engineering, Universiti Kebangsaan Malaysia, 43600 UKM, Bangi, Selangor*
[2]*Communications and Information Technology (ECIT) Queen's University Belfast, NI Science Park, Queen's Road, Queen's Island, Belfast BT3 9DT, United Kingdom*
Email: bahiah@vlsi.eng.ukm.my

ABSTRACT

The bandwidth limitation of a reflectarray is a consequence of the non-linear and high Q variation in the reflection phase which occurs when the element size is changed to produce the required progressive phase distribution across the antenna aperture. A significant increase in the bandwidth is shown to occur when the periodic structure of a grounded stacked rings or concentric rings generates two resonances which are closely spaced. This paper presents the reflection phase response of a two-layer array of orthogonally oriented concentric split rings for dual frequency broadband reflectarray. The concentric split ring concept is discussed in this chapter and the validity of the approach at X-band is confirmed by comparing the computed results, which is simulated by Micro-stripes™ simulator, and experimental results from waveguide simulator experiment. Good agreement is shown between the two sets of result. Simply by inserting gaps in the ring elements, it will suppress the interlayer coupling and produce polarisation sensitive scattering. The results demonstrate that these properties enable the reflection phase coefficients of a reflectarray to be independently optimised at two closely different frequencies.

Keywords: Concentric Ring, Dual Frequency, Dual Polarisation, Reflectarray Antenna

1. INTRODUCTION

A microstrip reflectarray antenna is an attractive alternative to conventional parabolic reflectors for many communication applications [1]. By using the reflection phase variation with element size relationship to create a suitable array layout, energy from the primary feed horn is transformed by the planar reflector to produce a focussed plane wavefront [1-2]. This however limits the antenna bandwidth to only few percent because the phase versus element size slope is generally large and non-linear at the extremities [1, 3].

It was shown that a concentric ring array can be designed to give a broader bandwidth than a single ring structure [4], and furthermore it is simpler to construct than the broadband stacked configuration described in [2-4]. However, this type of structure operates only over a single frequency range centred on the resonant frequency of either the inner or the outer ring [2]. This limitation applies to any type of dual resonant element [5] since the relative sizes of the two patches must be kept constant to provide the required reflection phase range and the linearity of the phase plot. However, dual frequency operation can be achieved by stacking two concentric ring elements, because each pair can be individually designed to generate the required phase response around the resonant frequency of either one of the two loops.

The required phase compensation which must be provided by a reflectarray element is determined by the progressive phase shift across the aperture which is dependent on the operating frequency of the antenna. This is given by the following equation,

$$\phi \text{ (deg)} = 360° \, \Delta L/\lambda \qquad (1)$$

where $\Delta L = L_2 - L_1$ is the path length difference between any two elements and λ is the wavelength.

The phase difference, ϕ between elements 1 and 2 depends on the path length difference ΔL, and it is a frequency dependent parameter. The phase difference can be compensated for by changing the physical size of the rings over the aperture, since this changes the reflection phase. For example, at the operating frequency of f_o, if the phase difference between two elements, ϕ is 90°, the size of element 2 must be designed to give a reflection phase coefficient which will lead the reflection phase of element 1 by 90°. If the operating frequency is increased to $2f_o$, Equation 1 shows that, the outer most element must be designed to give a phase lead of 180°. The physical size of the rings which is required to generate a plane wavefront is therefore different because of the frequency dependent self-resonant properties of the element and the differential path length.

A dual frequency antenna which consists of a two layer concentric ring array could be designed to generate the required response, however this would be subject to high interlayer coupling when the operating frequencies are closely spaced. High current which is generated in the active array, would excite the elements in the second periodic screen. This would therefore cause unwanted scattering from the reflectarray surface which may degrade the quality of the radiation pattern. To overcome this potential problem, a dual band reflecting surface has been designed using a two layer array of concentric split rings. In the split ring element concept, it was shown that by breaking the ring elements, the current distribution on the loop is modified and the mode excited is determined by the orientation of the incident **E**-vector. Therefore, since the resonant frequency of the split loop is polarisation dependent, unlike the continuous ring, this property is exploited to reduce the interlayer coupling which exists between the periodic arrays.

The dual polarisation dual frequency reflectarray shown in Figure 1 offers a cost effective method to manufacture a reflector antenna because operation over two frequency bands (which may be closely spaced) is provided by a single aperture.

2. DUAL POLARISATION CONCENTRIC SPLIT RING ARRAY CONCEPT

In principle, a two layer concentric ring array could provide dual frequency operation. However, the bands would
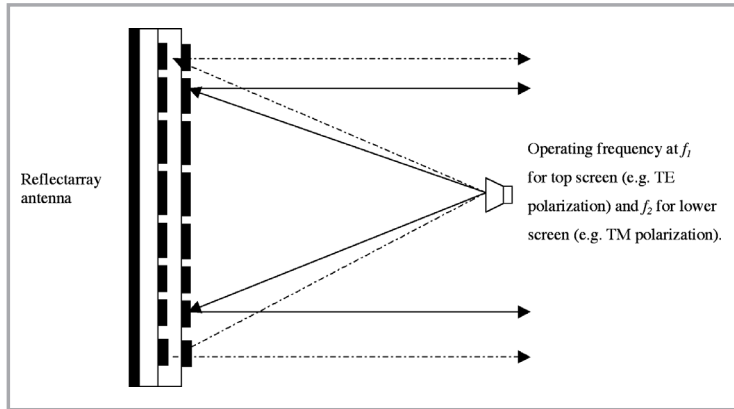
Figure 1: Dual polarisation dual frequency reflectarray antenna concept

need to be separated far enough apart to reduce interlayer coupling. To overcome this limitation, it is possible to use the polarisation sensitive properties of an array of concentric ring with the conductors broken at a suitable location. Square and circular loops are widely used as elements for frequency selective surfaces [6-7] and reflectarrays [8]. These loops are symmetrical and therefore, at normal incidence, the scattering parameters are insensitive to polarisation which means that the transmission coefficients are similar in the TE and TM planes. However, when the conductor is broken at a suitable location, the resonant frequency becomes a strong function of polarisation [9-10]. When the incident **E** vector is perpendicular to a single gap in the ring, the scattering parameters are similar to the continuous loop which resonates when the conductor length is approximately λ. However, a significant change occurs when the **E** field is oriented parallel to the gap. Here, two resonant modes are excited corresponding to loop lengths of approximately $\lambda/2$ and $3\lambda/2$. In this paper, this property has been exploited to create a reflectarray element which gives an autonomous reflection phase response at two closely spaced frequencies.

3. DUAL FREQUENCY DUAL POLARISATION ELEMENT DESIGN

The arrangement which is shown in Figure 2 consists of a grounded stacked array of two concentric split rings, where the individual periodic screens are designed to generate a prescribed phase shift at the centre frequency of one of the two operating bands. Figure 2 also shows that the elements in the two screens are offset by a rotation angle of 90° which effectively decouples the arrays, since in general, these will resonate at different frequencies for a given orientation of the incident **E** vector. For example, for TE polarisation, the rings on the upper surface resonate at the frequency when the loop length is λ, whereas the embedded rings resonate at the frequencies corresponding to loop lengths of $\lambda/2$ and $3\lambda/2$. The wavelength is dependent on the permittivity of the dielectric substrate and it is always smaller for the embedded rings. The upper array gives the prescribed phase shift in the TE plane at the centre frequency of one band, whereas the embedded array is designed to generate the required response at the centre of the second band, but in the TM plane. In both cases, the second screen is essentially decoupled since it resonates far from the design frequency of the active array.

4. SCATTERING BEHAVIOUR OF STACKED CONCENTRIC SPLIT RING ARRAY

The stacked concentric split ring element was designed using Micro-stripes [11] to resonate at centre frequencies of
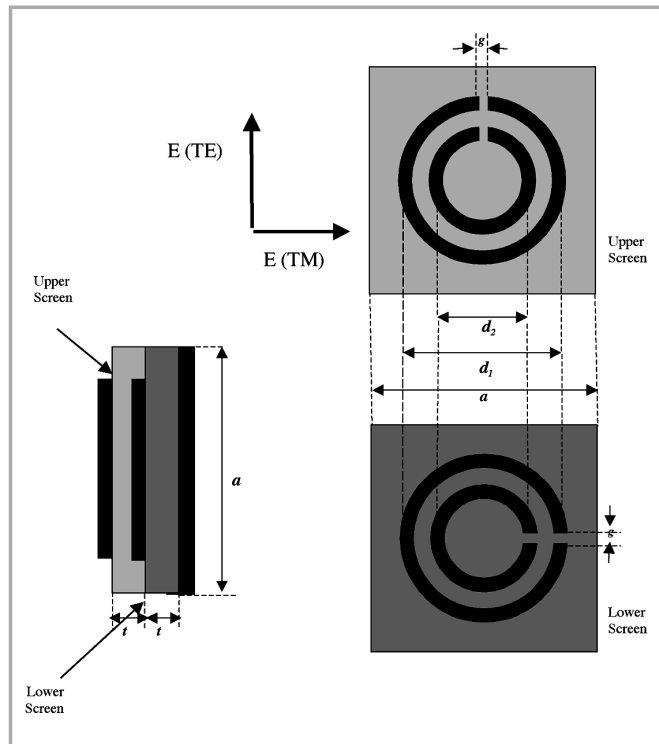

Figure 2: Periodic cell of reflectarray element
d_1 & d_2 = mean diameter of outer and inner ring (variable) respectively. I/O = d_2/d_1 = 0.86, a = 10 mm, ε_r = 3.54, tanδ = 0.0018, t = 1.524 mm, conductor width = 0.2 mm, gap size, g = 0.28 mm.

7.4 GHz for the lower screen and 8.9 GHz for the upper screen in the TM and TE plane respectively. To provide a good compromise between linearity and phase range, an inner to outer mean radius ratio (I/O) value of 0.86 was selected, since this provide the optimum design for the concentric continuous ring element [4]. The outer and inner radius of the rings on the two surfaces was chosen to be 3.0 mm and 2.58 mm respectively, the conductor width of each was 0.4 mm and the gap inserted in the patches was 0.28 mm. The ring elements were printed on a TACONIC [12] substrate of thickness 1.524 mm, ε_r = 3.54 and tan δ = 0.0018. The separation between the ground plane and the embedded periodic array and the rings on the upper surface was therefore 1.524 mm and 3.048 mm respectively.

The computer model shows that the stacked concentric continuous ring array cannot provide the required dual frequency operation because the results plotted in Figure 3 show that in the region around the lower resonance at 7.4 GHz, a large phase ripple is generated and the Q factor of the phase response of the outer ring on the lower surface is very large. Furthermore, the reflection phase range between 8.8-9.5 GHz (due to the excitation of the outer ring on the top screen) is significantly reduced by the resonance of the inner embedded ring around 8.8 GHz. Table 1 summarises the resonant frequencies of the individual nested loops.

Table 1: Predicted resonant frequencies of continuous concentric ring elements

	Upper screen	Lower screen
Inner ring (2.58 mm radius)	10.8 GHz	8.8 GHz
Outer ring (3.0 mm radius)	8.9 GHz	7.4 GHz

Clearly, the interlayer coupling is sufficiently large to degrade the phase plots around the operating frequencies of 7.4 GHz and 8.9 GHz. An alternative strategy must therefore be used to reduce the undesirable scattering from the array. This has been implemented by inserting gaps in the loop conductors to modify the current distribution and hence, give polarisation sensitive scattering from the surface.
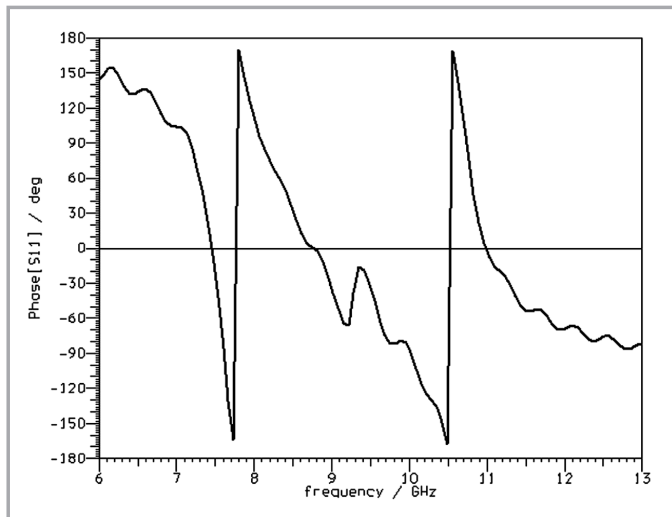

Figure 3: Predicted reflection phase response for a grounded stacked concentric continuous ring array structure

The behaviour of the stacked concentric split ring array element was predicted by exciting the loops on the upper screen with the incident **E**-vector normal to the gap (TE wave in Figure 2). In the computer model, the rings were printed on a 3.048 mm thick substrate, and the outer ring radius was chosen to resonate at 8.9 GHz. The choice of frequency enabled the S_{11} response to be measured using the waveguide simulator technique [13]. A second screen of the same size concentric split rings was embedded in the middle of the substrate at a distance 1.542 mm above the ground plane, and the gap was oriented at 90˚ relative to the rings on the upper surface (gap parallel to **E**-vector) to examine the effect on the phase response. The computed swept frequency reflection phase coefficients of both structures relative to a perfect conductor is shown in Figure 4 at normal incidence in the TE plane together with the measured results obtained from the waveguide simulator.

In the waveguide simulator measurement, the whole reflectarray is represented by only three rings array. The waveguide is constructed using a 30 x 10 mm rectangular aperture located at the end of 200 mm long flared rectangular waveguide. The flare angle is small to avoid the possibility of launching higher order modes. The infinite array is created because the elements are imaged on the perfectly conducting inner walls of the waveguide. In this work, the reflection phase is measured and calculated with respect to ground plane.

The outer and inner rings of the top surface resonate at 8.9 GHz and 10.8 GHz respectively, and around the former frequency, the phase response is shown to be very similar to the response when the lower periodic surface is removed. Scattering from the embedded array at the designed frequency (8.9 GHz) is insignificant because, in this plane, the rings resonate in the $\lambda/2$ current mode around 3.7 GHz (for the outer ring) and 4.3 GHz (for the inner ring), and at 10.7 GHz (for the outer ring) and 12.4 GHz (for the inner ring) in the $3\lambda/2$ mode as shown in Figure 5.
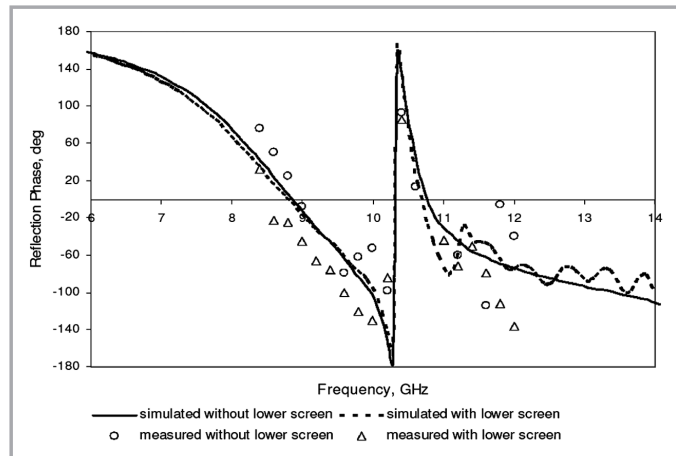

Figure 4: Simulated and measured reflection phase versus frequency at normal incidence in the TE plane with and without the lower screen
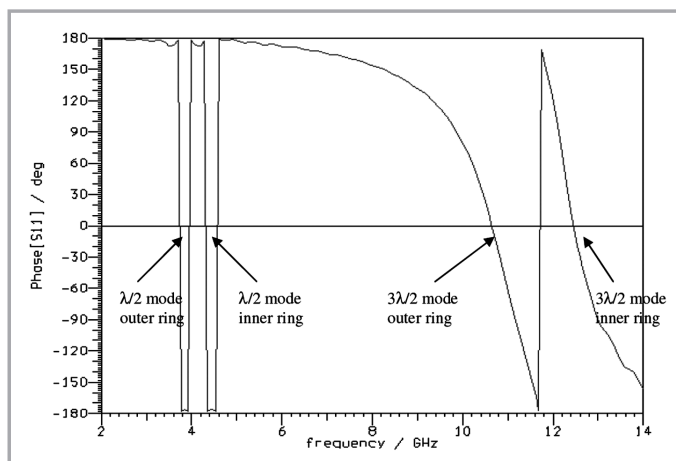

Figure 5: Simulated reflection phase versus frequency at normal incidence in TE plane for the lower screen with the top screen removed

In the computer model, the rings on the lower screen were then rotated by 90˚ so that the orientation of the gaps in the rings on the two surfaces was the same. The purpose of this was to observe the effect (if any) of an increase in the interlayer coupling. In this design, the two periodic screens resonate at similar frequencies; 8.8 GHz for the embedded inner ring and 8.9 GHz for the outer ring on the upper surface. Figure 6 shows that the resonant behaviour around 8.9 GHz is distorted by the high current which is excited in and reradiated by the inner ring of the embedded array. The computed swept frequency reflection phase response is shown to be in good agreement with the measured results obtained from the waveguide simulator experiments. The scattering from the surface plotted in Figure 6 is similar to the predicted results for the stacked concentric continuous ring array shown in Figure 3, because in this orientation, both pairs of split rings behave like a continuous loop which resonates when the conductor length is approximately λ. However, there is some trivial inconsistency between simulated and measured results around 8.4-9.0 GHz due to angle of incidence effect. In computer model, the wave is assumed at normal incident whereas the measurement, the incidence or scan angle of the simulated plane wave is a function of frequency.

The computed reflection phase response for the embedded periodic array for TM incidence is shown in Figure 7 with and without the periodic screen on the top surface of the array. In
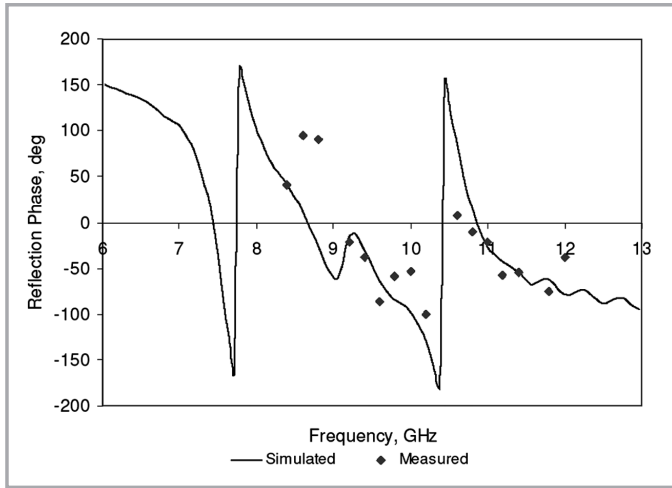
Figure 6: Simulated and measured reflection phase versus frequency in the TE plane for the same orientation of ring gaps on the top and lower screens
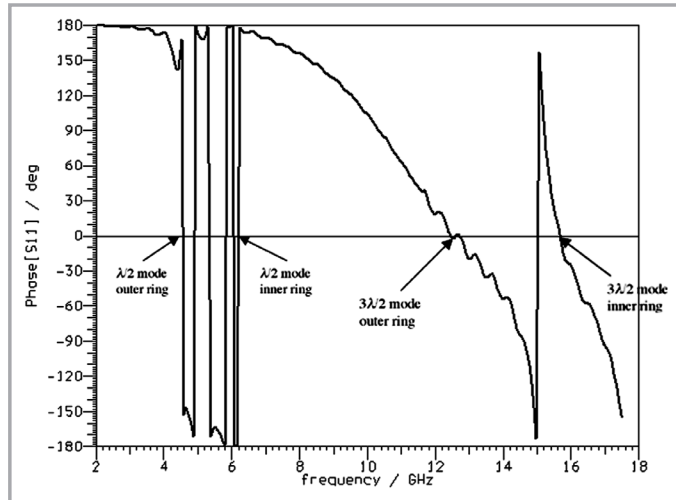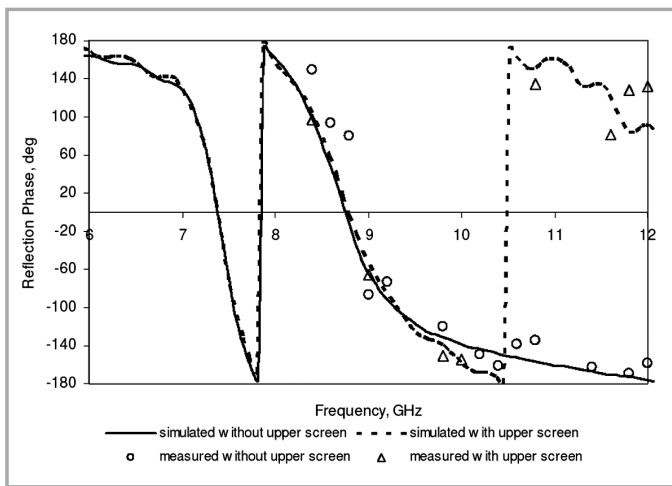

Figure 7: Simulated and measured reflection phase versus frequency at normal incidence in TM plane with and without the upper screen

Figure 8: Simulated reflection phase versus frequency at normal incidence in TM plane for the upper screen only
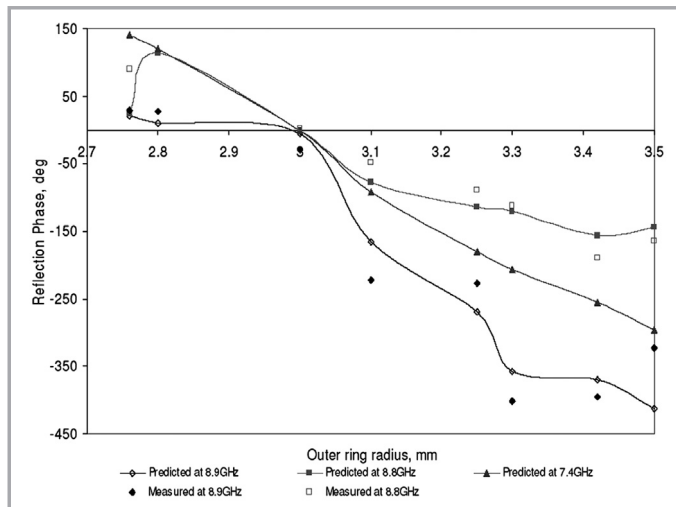

Figure 9: Measured and simulated reflection phase versus outer ring radius at normal incidence in the TE plane (8.9 GHz) and TM plane (7.4 GHz and 8.8 GHz)

this structure, the gaps inserted into the loops on the upper screen were offset by a rotation angle of 90° relative to those inserted into the loops on the lower screen. The measured results obtained from waveguide simulator experiments are also shown to be in good agreement with the computed results. The response of the structure around the lower resonant frequency (7.4 GHz) is unaffected by scattering from the upper screen because in the TM plane, the rings printed on this array resonate in the $\lambda/2$ current mode around 4.6 GHz and 5.3 GHz, and at 12.5 GHz and 15.7 GHz in the $3\lambda/2$ mode as shown in Figure 8 and Table 2. Therefore, the presence of the upper screen has very little effect on the scattering parameters of the embedded array around the centre design frequency of 7.4 GHz in the TM plane.

Table 2: Predicted resonant frequencies (GHz) of the split ring stacked array. (Operating frequencies of the antenna shown in bold)

Polarisation	Upper Screen	Lower Screen
TE	**8.9** & 10.8 (λ-mode)	10.7 & 12.4 ($3\lambda/2$-mode) 3.7 & 4.3 ($\lambda/2$-mode)
TM	12.5 & 15.7 ($3\lambda/2$-mode) 4.6 & 5.3 ($\lambda/2$-mode)	**7.4** & 8.8 (λ-mode)

5. REFLECTION PHASE VARIATION WITH RING SIZE

The reflection phase versus ring size plot was computed using Micro-stripes™ by varying the outer radius of the active array elements between 2.75 mm and 3.25 mm at 8.9 GHz in the TE plane, and 7.4 GHz in the TM plane. The orientation of the **E**-vector and ring gaps is shown in Figure 2. In the former model, the outer ring radius in the embedded screen was fixed at 3.0 mm, and at 7.4 GHz the same ring size was employed in the upper screen. The simulated results in Figure 9 show a reasonably smooth phase variation is obtained in both bands over a range, which exceeds 360°.

Experimental validation of the reflection phase range and linearity versus outer ring radius is also shown in Figure 9 at 8.9 GHz in the TE plane. The measurements at 7.4 GHz in the TM plane were not made because this is below the cut-off frequency of the waveguide simulator. Therefore, measurements and predictions were compared for the inner embedded ring at 8.8 GHz in TM plane since good agreement implies that the computed results at 7.4 GHz are also likely to be reliable. For operation at 8.8 GHz, an adequate phase range can only be achieved when the size of the rings is reduced, as shown in [2], because the results plotted in Figure 9 are for elements that are both inductive.

Table 3: Computed phase gradient and linear phase range for the stacked concentric split ring configurations at the two operating frequencies

Polarisation	Phase gradient (deg/μm)	Linear Phase range (deg)
TE (8.9GHz)	0.60	360°
TM (7.4GHz)	0.36	360°

Table 3 summarises the gradient and linear phase range for the concentric split ring design at the operating frequency of 8.9 GHz and 7.4 GHz in the TE and TM plane respectively. The results show that the response at 7.4 GHz gives a smaller phase slope (0.36°/μm) than the response at 8.9GHz (0.60°/μm), however the phase range is very similar and adequate for a reflectarray antenna design.

6. CONCLUSIONS

In this paper, polarisation sensitive scattering has been used to improve the performance of a dual frequency reflectarray element. Simply by inserting a gap in the conductors to modify the current distribution of the loops, and orientating the gaps orthogonally on the two screens, it is possible to decouple the arrays. These two periodic structures generally will resonate at different frequencies which are determined by the current mode and the electrical length of the loop. Measured results at X-band which are in close agreement with the computations, demonstrate that this approach can be used to enable the reflection phase coefficients of a reflectarray aperture to be independently optimised at two different frequencies. Decoupling the surface to give independent control of the reflection phase shift at two frequencies can simplify the design of the antenna where the different layouts on the two screens give stacked relative ring sizes (and hence resonant frequency separation) which vary over the scattering surface. ∎

REFERENCES

[1] Pozar, D.M., Targonski, S.D., and Syrigos, H.D., "*Design of millimeter wave microstrip reflectarrays*", IEEE Trans. Antennas Propag., 45, (2), pp. 287-295, 1997.

[2] Misran, N., Cahill, R., and Fusco, V.F., "*Reflection phase response of microstrip stacked ring elements*", Electron. Lett., 38, (8), pp. 356-357, 2002.

[3] Misran, N., Cahill, R., and Fusco, V.F., "*Performance of a broadband ring element reflectarray*", IEEE 2003 High Frequency Postgraduate Student Colloquium, pp. 111-114, 2003.

[4] Misran, N., Cahill, R., and Fusco, V.F., "*Design optimisation of ring elements for broadband reflectarray antennas*", Proc. IEE Microwaves Antennas and Propagation, 150, (6), pp. 440-444, 2003.

[5] Encinar, J.A., "*Design of a dual frequency reflectarray using microstrip stacked patches of variable size*", Electron. Lett., 32, (12), pp.1049-1050, 1996.

[6] Vardaxoglou, J.C. 'Frequency Selective Surfaces – Analysis and Design', John Wiley, Research Studies Press Ltd, 1997.

[7] Parker, E.A., and Hamdy, S.M., "*Rings elements for frequency selective surfaces*", Electronics Letters, Vol. 17, pp. 612-614, August 1982.

[8] Guo, Y.J., and Barton, S.K., "*Phase correcting zonal reflector incorporating rings*", IEEE Trans. Antennas Propagat., vol. 43, pp. 350-355, April 1995.

[9] Chirpin, A.D., Parker, E.A., and Batchelor, J.C., "*Resonant frequencies of open and closed loop frequency selective surface arrays*", Electron. Lett., 36, (19), pp. 1601-1602, 2000.

[10] Chulmin, H., and Chang, K., "*Ka-band reflectarray using ring elements*", Electron. Lett., 39, (6), pp. 491-493, 2003.

[11] MICROSTRIPES is a Trademark software product of FLOMERICS, www.flomerics.com

[12] TACONIC, www.taconic-add.com. (accessed 20 July 2006)

[13] Hannan, P.W., and Balfour, M.A., "*Simulation of a phased-array antenna in waveguide*", IEEE Trans. Antennas Propag., 13, (3), pp. 342-343, 1965.

PROFILES

Norbahiah Misran
Electrical, Electronic and System Engineering Department
Faculty of Engineering
Universiti Kebangsaan Malaysia
43600 UKM, Bangi
Selangor Darul Ehsan

Robert Cahill
Communications and Information Technology (ECIT)
Queen's University Belfast
NI Science Park, Queen's Road
Queen's Island, Belfast BT3 9DT,
United Kingdom